

Preparation of Hollow Poly(imino ether ketone) Microspheres by Microliquid Technique

Guanjun Chang,¹ Lubin Miao,^{1,2} Zhen Xu,^{1,2} Yi Xu,^{1,3} Lidong Wei,^{1,2} Hongju Hu,^{1,3} Xuan Luo,¹ Lin Zhang,¹ Runxiong Lin²

¹Research Center of Laser Fusion, China Academy of Engineering Physics, Mianyang 621900, China

²Engineering Research Center of High Performance Polymer and Molding Technology, Ministry of Education, Qingdao University of Science and Technology, Qingdao 266042, China

³School of Materials Science and Engineering, Southwest University of Science and Technology, Mianyang 621010, China

Received 11 November 2010; accepted 26 May 2011

DOI 10.1002/app.35007

Published online 29 November 2011 in Wiley Online Library (wileyonlinelibrary.com).

ABSTRACT: 1, 4-bis (4-amiophenoxy) benzene and 1, 4-Bis (4-bromobenzoyl) benzene as monomers, poly(imino ether ketone) (PIEK) was synthesized via palladium-catalyzed aryl amination reaction. Based on the good chemical and physical properties, big diameter (0.6–2 mm) hollow microspheres of PIEK, used for Inertial Confinement Fusion research, were prepared by using the microliquid technique and double-layer latex technique. A new double T-channel droplet generator was designed and developed for fabrication of controlled-size PIEK hollow microspheres continuously. Study on manipulative condition of diameter and thickness of microspheres was done, and density matching

impacting on the quality of shells was discussed. The structures of the PIEK hollow microspheres were characterized, and they possessed equal wall thickness and good spherical symmetry. The properties of the microspheres were detected, and the results showed that they showed good stability under cold environment and high temperature. Additionally, the PIEK hollow microspheres exhibited good mechanical and anti-irradiation properties. © 2011 Wiley Periodicals, Inc. *J Appl Polym Sci* 124: 4061–4069, 2012

Key words: poly(imino ether ketone); hollow microspheres; micro-liquid technique

INTRODUCTION

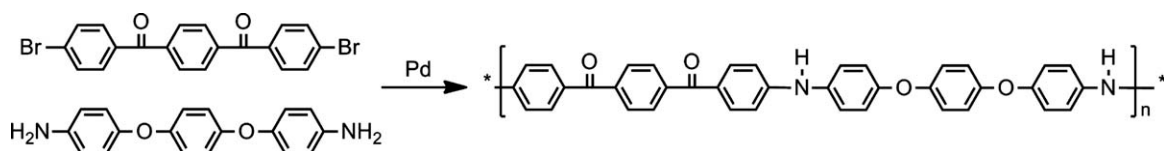
Hollow microsphere has a wide range of application in science, technology, and medicine, such as controlled release of drugs, carbon-less copy paper, impact modifiers, and photonic molecules.¹ Since John Nuckolls of the Lawrence Livermore National Laboratory (LLNL) first published the theory of high density nuclear fusion in 1972.² The focus of Inertial Confinement Fusion (ICF) research was shifted to pellet fusion with multibeam laser irradiation under high compression. For the above reason, study on fabrication of hollow microspheres occupy a very important position in ICF research, and the preparation of hollow polymeric microsphere has been one of the core technologies in ICF research both here and abroad. The usual polymers used for ICF pellet are polystyrene (PS), polyvinyl alcohol (PVA), polyvinyl acetate (PVAC), and polyacrylonitrile (PAN).^{3–5} However, owing to the technological upgrading development of ICF, especially in low temperature environment, there is a higher demand for properties of hollow polymeric microspheres used for ICF pellet,

such as high tensile strength, high elastic modulus, low thermal expansion coefficient, high/low temperature resistance, and good solubility. The polymers mentioned above cannot meet the demand.

Polyimide (PI) is one of the most important high performance polymers.^{6,7} Because of their good thermal stability, excellent mechanical properties in cryogenic deuterium/tritium (DT) fuel, and optical activities added to solid DT, currently PI became one of the leading materials for ICF pellet.⁸ In 1995, the scientists from LLNL suggested that PI could be used for the pellet. The following year, hollow PI microsphere for direct ICF research was obtained by researchers from the University of Rochester. Within the past decades, the preparation and assembly method have made remarkable progress, the method combining of CVD, imination and mandrel degradation was confirmed as the preparation process of PI hollow microsphere. Processes of mandrel cleaning and high temperature preprocessing followed by imination were provided to improve the surface quality of hollow PI microspheres. However, the whole process is complicated for operation. Furthermore, during the process of imidization there was water connected with poly(amic acid)s by hydrogen bonding, it was difficult to emanate the water completely, which led to pinhole structure of the products and affected the precision and the properties.

To solve the problems above, the scientists try to find the solutions, such as, synthesizing soluble

Correspondence to: L. Zhang (zhlmy@sina.com)R. Lin (qdlrx@qust.edu.cn).



Scheme 1 The structure of PIEK.

PI,^{9,10} using microliquid technique in place of CVD to fabricate hollow PI microspheres; synthesizing novel high performance polymers, taking synthesized polymers as raw material, fabricating new high performance hollow polymer microspheres. Poly(imino ether ketone)s (PIEKs) as the new high performance polymers have been synthesized, whose properties were similar to the PI.¹¹ Compared with PI, PIEK also has such virtues as these: (1) PIEK could be easily dissolved in organic solvents, therefore, can use microliquid technique to fabricate PIEK hollow microspheres with sample preparation simple; (2) Dehydration of macromolecule did not occur during hollow microsphere drying process, and high quality PIEK hollow microspheres could be fabricated. In this article, a new double T-channel droplet generator was designed and developed, and PIEK hollow microspheres have been fabricated through micro-liquid technique. The poly hollow microspheres can be considered as a growing new type of high performance ICF pellet.

EXPERIMENTAL SECTION

Materials and instruments

Materials

N,N-dimethylacetamide (DMAc) was purchased from Tianjin Kermel Chemical Reagent Co., AR. Chengdu, Polydimethyl silicone was purchased from Chen Guang Research Institute of Chemical Industry, Tianjin, Purity > 98%, Kinematic viscosity (25°C):100 mm² s⁻¹, density: 0.971 g cm⁻³. PIEK was synthesized in our laboratory, Purity > 99%.

Instruments

FTIR spectrum was recorded on a Nicolet 6700 FTIR spectrometer. Elemental analysis was performed on a Perkin-Elmer model 2400 CHN analyzer. ¹H-NMR spectrum was recorded using Bruker AMX500 Hz NMR spectrometers in DMSO-*d*₆. Syringe Pump (TJ-3A/W0109-1B), Baoding Lange Constant Flow Pump Co. Digital mechanical agitator (RW 20), IKA, Germany. Tension Meter (Sigma700), KSV Co., Finland; X-ray imager was designed in our laboratory.

Synthesis of PIEK

An oven-dried resealable two-neck 100-mL flask equipped with magnetic stirrer, a nitrogen outlet, inlet, and water-cooled condenser, added to which are tris(dibenzylideneacetone)dipalladium(0) Pd₂(dba)₃ (0.10 mmol), BINAP (0.30 mmol), 1,4-bis(4-aminophenoxy) benzene (10.0 mmol), and dimethylacetamide (15 mL). The reaction mixture was flushed with high purity nitrogen. This procedure was repeated three times. The flask was immersed in a 60°C oil bath for 2 h. Then, primary aromatic 1,4-Bis(4-bromobenzoyl)benzene (10.0 mmol) and sodium tert-butoxide (NaOt-Bu) (20.0 mmol) were added, and the reaction mixture was heated to 100°C for 2 h and then to 170°C for 6 h with continuous stirring. The resulting in polymer solution was allowed to slowly cool down to room temperature and precipitated into water, filtered, and then dried at 100°C under vacuum.

The structure of the polymer synthesized was shown in Scheme 1, and the main properties were listed in Table I.

PIEK was characterized by FTIR, ¹H-NMR, and elemental analysis. The results showed good agreement with the proposed structure. As an example, the ¹H-NMR spectrum of PIEK is shown in Figure 1.

Fabrication of PIEK hollow microspheres

Micro-liquid technique is a rising laboratory technique that has been widely used in bioscience and analytical chemistry. Researchers at Osaka University had prepared PS hollow microspheres (2–7 mm in diameter) by microencapsulation technology.¹² As McQuillan¹³ designed droplet generator for the preparation of ICF mandrel material, Norimatsu and

TABLE I
Main Properties of Poly(imino ether ketone)

| <i>M_n</i> (g/mol) ^a | <i>M_w</i> (g/mol) ^a | <i>M_w</i> / <i>M_n</i> ^b | <i>T_g</i> (°C) | <i>T₅</i> ^c (°C) | <i>T₅₀</i> ^d (°C) | [η] ^e (g/dL) |
|--|--|---|------------------------------|---|--|----------------------------|
| 51,400 | 120,700 | 2.35 | 209 | 470 | 700 | 0.468 |

^a By GPC (calibrated by polystyrene standards).

^b Polydispersity index.

^c *T*₅: temperature of 5% weight loss.

^d *T*₅₀: temperature of 50% weight loss.

^e [η] intrinsic viscosity measured at 25°C in DMF.

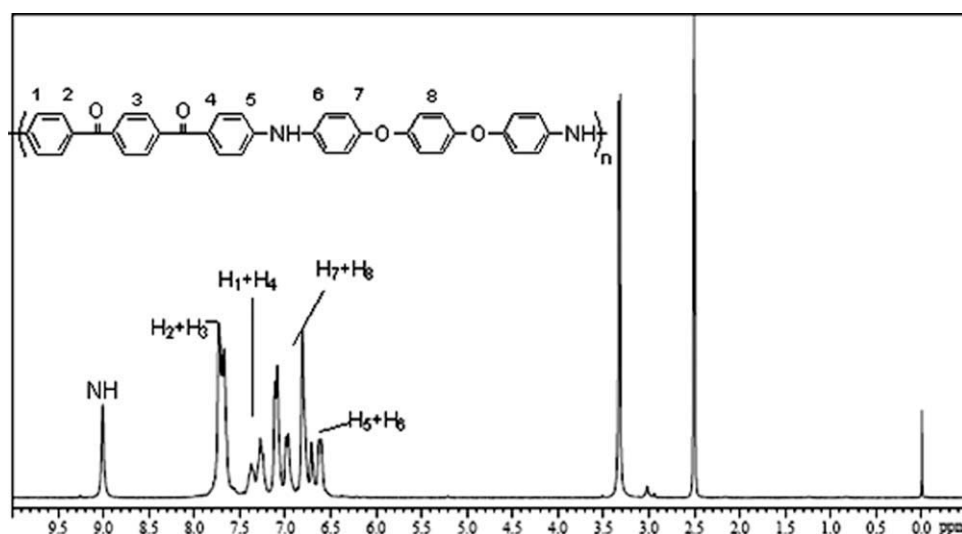


Figure 1 $^1\text{H-NMR}$ (500 MHz) spectrum of P-11 recorded in $\text{DMSO-}d$.

Nagai¹⁴ continued this study. Now, this technology was simple and easy to control. Derived technologies (three nozzles technology, microchannel technology, and so on.) are developed also. Figure 2 illustrated the new double-T channels emulsification system which was developed in recent years.¹⁵ It was found experimentally that at the first T-type passage, the oil phase packed the water phase to achieve emulsion; however, at the second T-type passage emulsion, it did not have the desired effect look like the scene showed in Figure 2. This was because the oil phase is prone to adhering the inner wall, which results in demulsification, so the double emulsion of assembling cannot be achieved.

Based on the observations, we designed triple-orifice droplet generator (Fig. 3), which was used to fabricate PIEK hollow microspheres. By changing the direction of channel, and due to the shear flow between S phase and Oo phase, Oi/S emulsion particles detached from the nozzle, a stable double emulsion could be obtained.

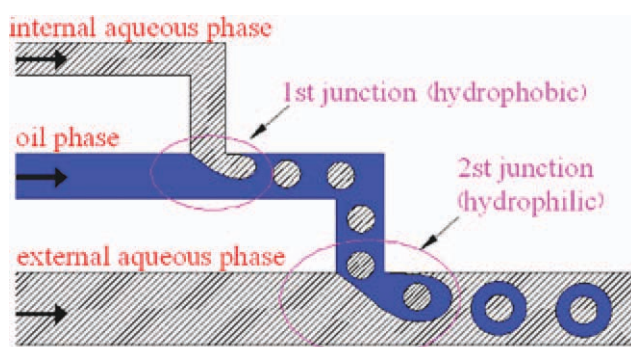


Figure 2 The sketch double-T channels [Color figure can be viewed in the online issue, which is available at wileyonlinelibrary.com].

Density matching control

Figure 4 illustrated the strength of the droplet in the solvent. There were mainly three forces to droplets in the solution: liquid droplet gravity, buoyancy force, and viscous resistance. According to formula of gravity, viscous resistance, and buoyancy force, the following equations could be deduced.

$$F = W - U \quad (1)$$

$$6\pi\eta av = \frac{4}{3}\pi R^3(\rho - \sigma)g \quad (2)$$

$$v = \frac{2(\rho - \sigma)R^2g}{9\eta} \quad (3)$$

$$v = KR^2 \quad (4)$$

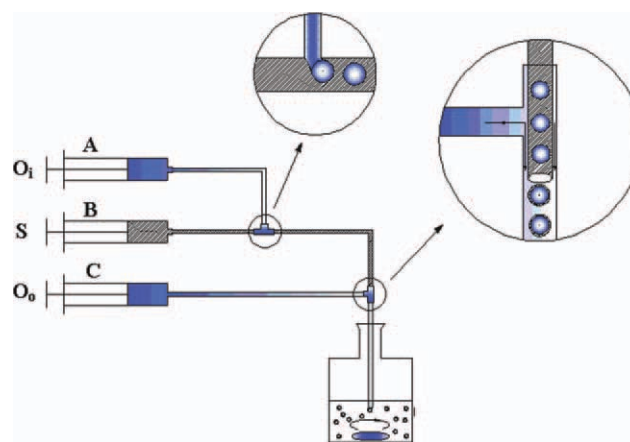


Figure 3 The sketch of actual channels droplet generator. (S phase: PIEK in DMAc solution, 2–3 wt %, $\rho = 0.956 \text{ g cm}^{-3}$. Oo and Oi phase: polydimethyl silicone) [Color figure can be viewed in the online issue, which is available at wileyonlinelibrary.com].

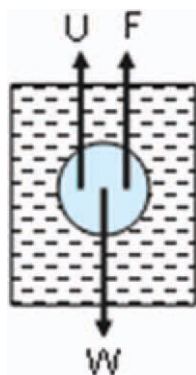


Figure 4 Forces impact on the droplet in solvent [Color figure can be viewed in the online issue, which is available at wileyonlinelibrary.com].

$$K = \frac{2(\rho - \sigma)g}{9\eta} \quad (5)$$

In formula (1), where F , W , and U were, respectively, viscous resistance, droplet gravity, and buoyancy force to droplet. In formula (2), where v , ρ , σ , η , R , g , and K were, respectively, falling rate of liquid droplet, liquid droplet density, solution density, viscous resistance of solution, semidiameter of liquid droplet, gravity acceleration, and coefficient of relationship between drop diameter and descending speed. When $\rho = \sigma$, the resultant force of droplet was zero. As the forces on opposite sides were equal and opposite, the droplet suspended in the still solution. From this, density matching had great influence of emulsion stability and liquid droplet sphericity. Sedimentation of droplets in the solution and emulsion separation are restrained as well. When the solution temperature was 25°C, the density of solution may have different result which varies from different concentration of PIEK in DMAc solutions referred in Table II. Table III showed the density of O phase and S phase (concentration 0.02 g mL⁻¹) which varied with temperature, and the change of η and K values in the O phase with temperature. When the concentration was 0.02 g mL⁻¹, the density of PIEK solution and O phase decreased with the temperature increasing, but the density difference of two fluids in the low-temperature region less than the one in the high temperature. The viscous

TABLE II
Density of DMAc Solution with Different PIEK Concentration (25°C)

| Concentration (g/mL) | 0 | 0.01 | 0.02 | 0.03 | 0.04 | 0.05 |
|------------------------------|-------|-------|-------|-------|-------|-------|
| Density (g/cm ³) | 0.946 | 0.949 | 0.956 | 0.961 | 0.966 | 0.971 |

coefficient of PDMS decreased with the temperature increasing also. Using the above formula, calculate K , (1)–(5), it was found that K value increased as the temperature increased.

By using K value and formula (1), the liquid droplets with descent calculated rates, whose diameters varied from 0.1 mm to 6 mm were obtained at different temperature, as indicated in Figure 5. When the semidiameter was less than 1 mm, the temperature had little effect on the settlement rate of droplets, meanwhile, the radius had little effect on the settlement rate of droplets also. When the semidiameter was larger than 1 mm, the effect of temperature gradually increased to the settlement rate of droplets, the effect of radius did so as well.

Dimension

When the equipment of double microemulsion was installed, and the formula of three-phase solution was defined, Oi phase flow rate, S phase flow rate, and the PIEK concentration could be adjusted and the diameters as well as wall thicknesses of PIEK hollow microsphere could be controlled.

If other factors were certain, when Oo-phase flow rate increased, the diameters and thicknesses of hollow microsphere decreased, as shown in Figure 6. When PDMS flew through the second T-type in Oo-phase, the flow rate increased, which resulted in shorter forming time of S/Oi emulsion. Meanwhile, when Oi-phase flow rate and S-phase flow rate were certain, it resulted in extrusion rate of S/Oi microemulsion being certain. Above all, the volume of microemulsion decreased as PDMS flow rate in the Oo-phase increased. As shown in Figure 6, when $C_{PIEKs} = 0.02$ g mL⁻¹, $V_S = 10$ mL h⁻¹, $V_{Oi} = 16$ mL h⁻¹, and at different V_{Oo} , the maximum diameter of PIEK hollow microsphere was about 1500 μ m, the maximum wall thickness was about 26 μ m, the

TABLE III
Density of O and S (0.02g/mL), η Value of O and K Value at Different Temperature

| Temperature (°C) | | 20 | 25 | 30 | 35 | 40 | 45 | 50 | 55 | 60 |
|------------------------------|-----------------------------|-------|-------|-------|-------|-------|-------|-------|-------|-------|
| Density (g/cm ³) | O | 0.975 | 0.971 | 0.966 | 0.962 | 0.958 | 0.954 | 0.949 | 0.945 | 0.941 |
| | S | 0.960 | 0.956 | 0.952 | 0.948 | 0.943 | 0.938 | 0.934 | 0.930 | 0.925 |
| | $\Delta\rho$ | 0.015 | 0.015 | 0.014 | 0.014 | 0.015 | 0.016 | 0.015 | 0.015 | 0.016 |
| η | | 0.569 | 0.510 | 0.468 | 0.430 | 0.399 | 0.369 | 0.336 | 0.316 | 0.285 |
| | K ((s mm) ⁻¹) | 5.74 | 6.41 | 6.52 | 7.09 | 8.19 | 9.44 | 9.72 | 10.34 | 12.23 |

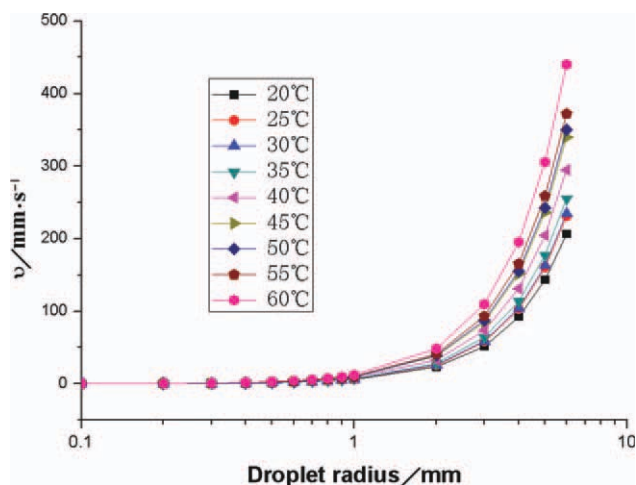


Figure 5 Droplet dimension impact on subsiding speed at different temperatures [Color figure can be viewed in the online issue, which is available at [wileyonlinelibrary.com](#)].

minimum diameter was about 670 μm , the minimum wall thickness was about 7 μm .

When S-phase concentration and V_{O_0} value were constant, liquid droplets of the second T-type had same diameter, the ratio of volume of the two phase reassigned as V_S and V_{O_i} changed. In this article, to simplify calculation, $V_S + V_{O_i}$ were constant, $\lambda = V_S/V_{O_i}$ was variable. When λ increased, the diameter of PIEK hollow microsphere decreased, and the wall thickness of PIEK hollow microsphere increased, as shown in Figure 7. When the λ increased, the volume of S-phase increased (PIEK increased), then wall thickness of microsphere increased, meanwhile, the volume of O_i -phase increased, which led to decreasing of microsphere volume. When $C_{\text{PIEK}_S} = 0.02 \text{ g mL}^{-1}$, $V_{O_0} = 100 \text{ mL h}^{-1}$, $V_S + V_{O_i} = 100 \text{ mL h}^{-1}$, and λ was variable, the maximum diameter of PIEK hollow microsphere

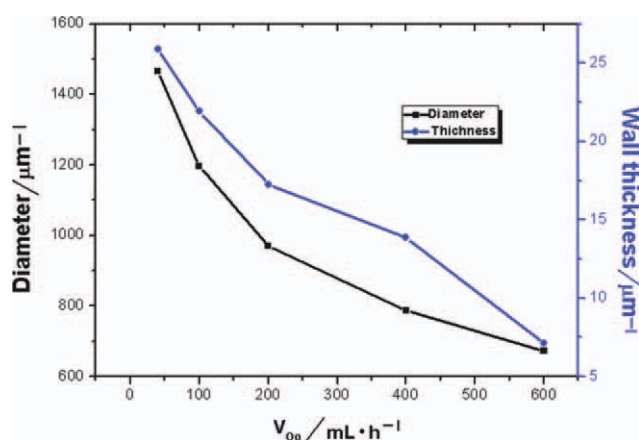


Figure 6 Diameter and thickness of PIEK hollow microspheres in change of V_{O_0} [Color figure can be viewed in the online issue, which is available at [wileyonlinelibrary.com](#)].

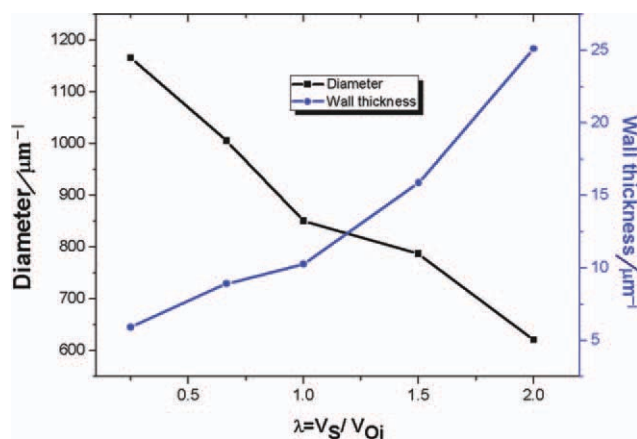


Figure 7 Diameter and thickness of PIEK hollow microspheres in change of V_S [Color figure can be viewed in the online issue, which is available at [wileyonlinelibrary.com](#)].

was about 1117 μm , and the wall thickness was about 6 μm , the minimum diameter was about 621 μm , and the wall thickness was about 26 μm .

When the third-phase flow rate was constant and the concentration of PIEK increased, the diameter and the wall thickness of hollow microsphere increased also, as shown in Figure 8. That was because the emulsion size was constant, the concentration of PIEK decreased, and the DMAc solution increased. On the grounds of solution viscosity, density matching, and emulsion stability, the regulating concentration of PIEK varied from 0.01 to 0.04 g mL^{-1} . When the concentration of PIEK was less than 0.01 g mL^{-1} , the hollow microspheres were easily broken during drying process. When the concentration of PIEK was larger than 0.04 g mL^{-1} , the viscosity of microspheres increased, which led to density mismatching and pipeline plugging. According to Figure 8, when $V_{O_0} = 100 \text{ mL h}^{-1}$, $V_S = 50 \text{ mL h}^{-1}$, $V_{O_i} = 50 \text{ mL h}^{-1}$ with variable C_{PIEK_S} , the maximum

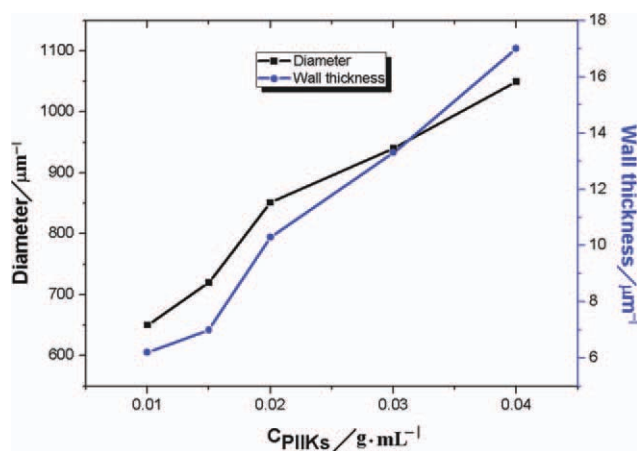


Figure 8 C_{PIEK_S} impact on the diameter and thickness of PIEK hollow microspheres [Color figure can be viewed in the online issue, which is available at [wileyonlinelibrary.com](#)].

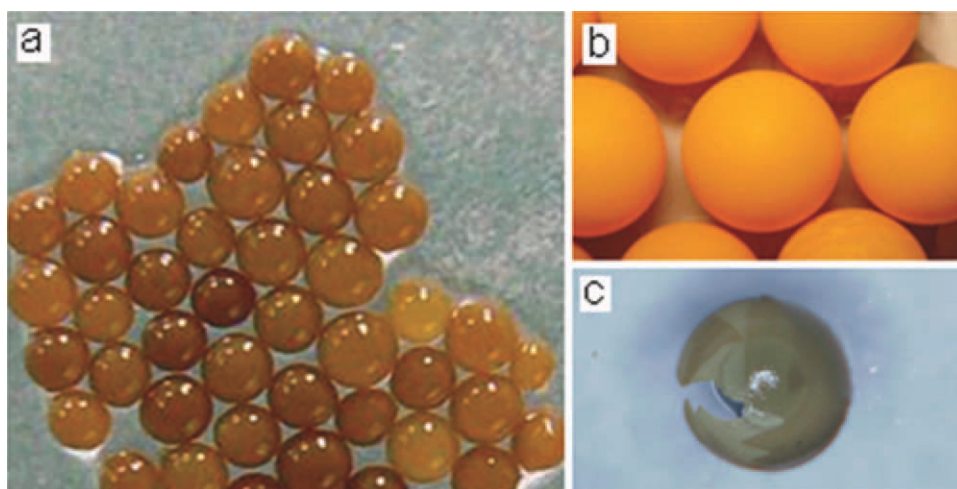


Figure 9 Optical microscope images of PIEK hollow microspheres [Color figure can be viewed in the online issue, which is available at wileyonlinelibrary.com].

diameter of PIEK hollow microsphere was about 1050 μm , and the wall thickness was about 17 μm , the minimum diameter was about 650 μm , and the wall thickness was about 6 μm .

THE STRUCTURES AND THE PROPERTIES OF PIEK HOLLOW MICROSPHERES

Structures

When the conditions of this experiment were determined, the size of emulsion was same. Because of the protection of Oo phase, PIEK emulsions would not mix together. During dissolution and diffusion of DMAc, equivalent DMAc diffused into the external system, the ultimate size of PIEK was almost the same. When $V_{Oo} = 300 \text{ mL h}^{-1}$, $V_S = 50 \text{ mL h}^{-1}$, $V_{O_i} = 50 \text{ mL h}^{-1}$, $C_{PIEK} = 0.02 \text{ g mL}^{-1}$, one batch of PIEK hollow microspheres were obtained by Optical microscope, as shown in Figure 9. The mean diameter of microspheres was 716.7

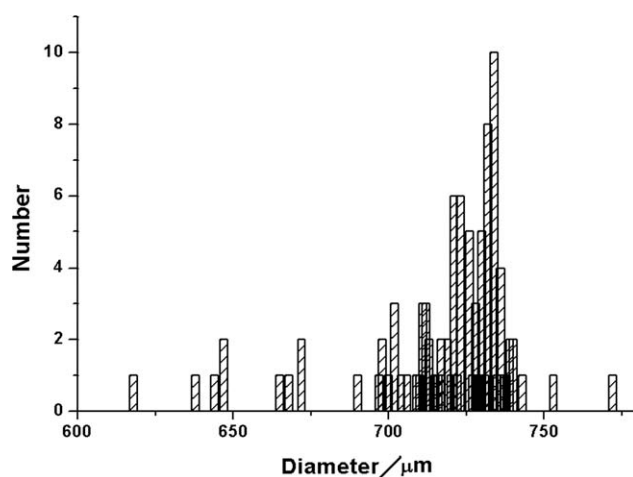


Figure 10 Diameter distribution of one batch of PIEK hollow microspheres.

μm (standard deviation was 31 μm), and up to 88% of microspheres had diameter between 700 to 750 μm (Fig. 10). In Table IV, it showed the wall thicknesses of seven randomly picked microspheres. According to data analysis, the microspheres' mean wall thickness was 14.1 μm (standard deviation was 1.28 μm). X-ray image of different wall thicknesses of microsphere was shown in Figure 11, Figure 11(a) represented the microspheres whose mean diameter was 10 μm , Figure 11(b) represented microspheres whose mean diameter was 20 μm , and Figure 11(b) represented the microspheres whose mean diameter was 40 μm . They all had equal wall thickness.

Circularity analysis

The plasma was compressed in ICF research, so it demanded the fuel containers to be highly spherical symmetry. Because of this, following were the analysis results of PIEK hollow microsphere samples, which were analyzed by using out-of-roundness of hollow microsphere. As shown in Figure 12, hollow microsphere diameter is measured in three directions and each angle is 45°. The difference between the highest and lowest value of the three is the out-of-roundness of hollow microsphere. The hollow microspheres were sampled in randomly, seven of them were shown in Table V. The results showed that out-of-roundness was less than 8.05 μm in this group.

TABLE IV
Thickness of PIEK Hollow Microspheres

| Numbering | 1# | 2# | 3# | 4# | 5# | 6# | 7# | Mean value | Standard deviation |
|----------------------------------|------|------|------|------|------|------|------|------------|--------------------|
| Wall thickness (μm) | 11.7 | 13.2 | 14.0 | 14.5 | 14.9 | 15.1 | 15.3 | 14.10 | 1.28 |

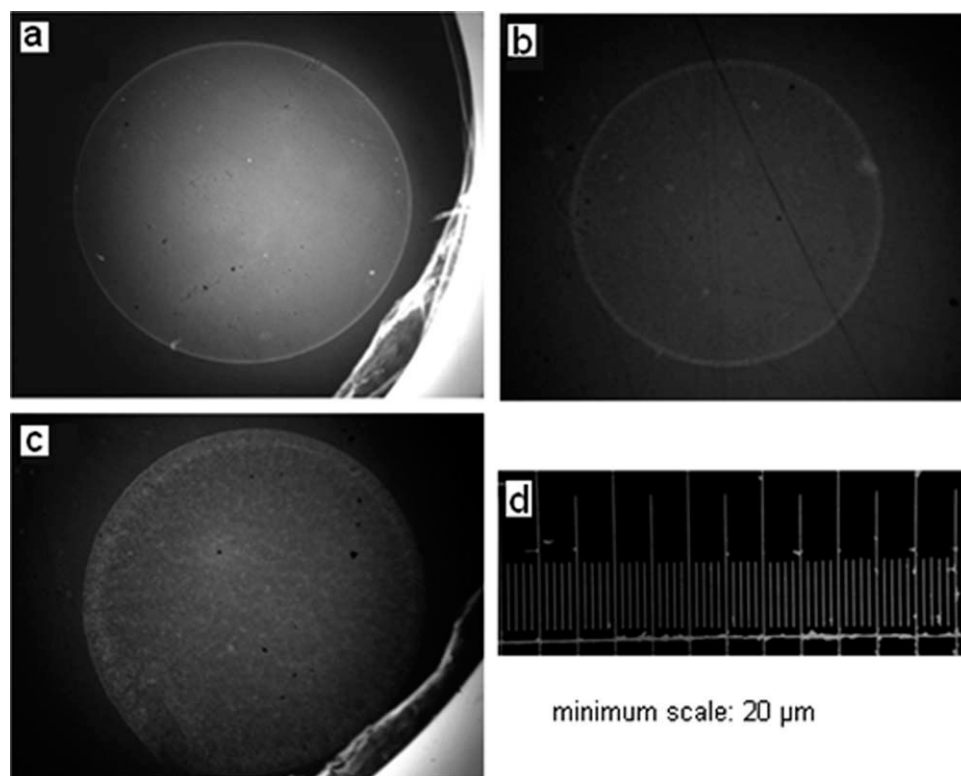


Figure 11 X-ray photograph of PIEK hollow microspheres with different thicknesses. (a: 10 μm , b: 20 μm , c: 40 μm , and d: ruler).

Thermal analysis

Thermal distortion temperature of the PIEK hollow microspheres determines its application scope. On account of the peculiar structure of spherical shell of polymeric hollow microsphere, the behavior of thermal distortion temperature is different between the PIEK hollow microspheres and the PIEK matrix material. The PIEK hollow microspheres were placed on the thermal polarizing microscope, and Figure 13 showed the tendency of ratio of diameter contraction increases with the temperature (heating rate: 10 min^{-1} , temperature range: -190°C – 600°C).

According to Figure 13, the contraction of PIEK hollow microspheres was divided into four stages. As shown in Figure 14, at the first stage (room temperature $\sim -190^\circ\text{C}$), expansion rate of the microsphere was about 0.6%. But in general, the PIEK hollow microspheres were in a good state of preservation, when they are in low temperature environment. At the second stage (room temperature $\sim 280^\circ\text{C}$), contraction rate of the microsphere was less 2.0% [Fig. 15(a,b)]. At the third stage (room $280 \sim 450^\circ\text{C}$), microsphere has greater contraction deformation rate up to 55%. Despite that, the microsphere still retains its hollow feature [Fig. 15(c)]. At the fourth stage (large than 450°C), the microsphere contracted quickly with rising temperature, which resulted in rupture of the hollow feature [Fig. 15(d)].

Mechanical properties

As a material of ICF pellet, PIEK hollow microspheres should absorb a certain amount of inflation pressure. In this article, three groups of hollow microspheres (the wall thicknesses were 10 μm , 20 μm , and 40 μm , respectively) were filled with nitrogen, and inflation pressure of PIEK hollow microspheres was detected. The results were shown in

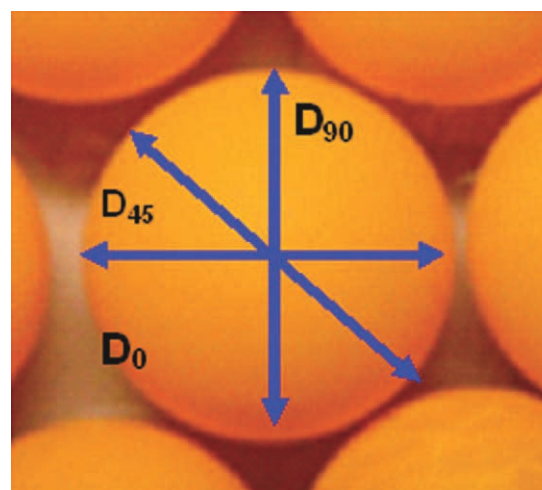


Figure 12 The instrumentation plan of out-of-roundness of PIEK hollow microspheres [Color figure can be viewed in the online issue, which is available at wileyonlinelibrary.com].

TABLE V
The Out-of-Roundness Analysis of PIEK Hollow Microspheres

| Microspheres no. | 1 | 2 | 3 | 4 | 5 | 6 | 7 |
|----------------------------|--------|--------|--------|--------|--------|--------|--------|
| D_0 (μm) | 868.09 | 827.66 | 872.72 | 844.68 | 931.91 | 797.87 | 831.91 |
| D_{45} (μm) | 873.12 | 830.23 | 874.01 | 848.22 | 936.23 | 796.31 | 833.10 |
| D_{90} (μm) | 872.34 | 822.28 | 865.96 | 842.55 | 938.68 | 791.49 | 827.67 |
| Out-of-roundness | 5.03 | 7.95 | 8.05 | 5.67 | 7.77 | 6.38 | 5.33 |

Table VI. From the results, one could see that the more wall thickness increased, the more pressure PIEK hollow microspheres absorbed. Thick wall hollow microspheres could absorb high pressure; however, they could influence the energy gain of ICF as well. However, at the present time, the mechanical property of PI hollow microspheres is better than PIEK hollow microspheres dose.

CONCLUSIONS

PIEK was synthesized by the condensation polymerization of 1,4-bis(4-amiophenoxy) benzene with 1,4-Bis(4-bromobenzoyl)benzene via palladium-catalyzed aryl amination reaction. A new double T-channel droplet generator, which was simple and easy to

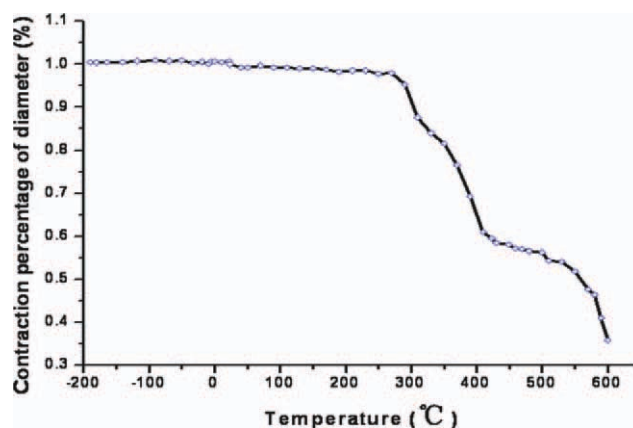


Figure 13 PIEK hollow microspheres contraction at different temperature [Color figure can be viewed in the online issue, which is available at wileyonlinelibrary.com].

control, was designed and developed for PIEK hollow microspheres fabrication. Used micro-liquid and double-layer latex techniques, various of PIEK hollow microspheres with different diameter (0.6–2 mm) and different thicknesses (10–40 μm) were fabricated through adjustment the process parameters, and PIEK hollow microspheres prepared showed equal wall thickness and good spherical symmetry. Additionally, they possessed good stability in cold environment or at high temperature. The mechanical

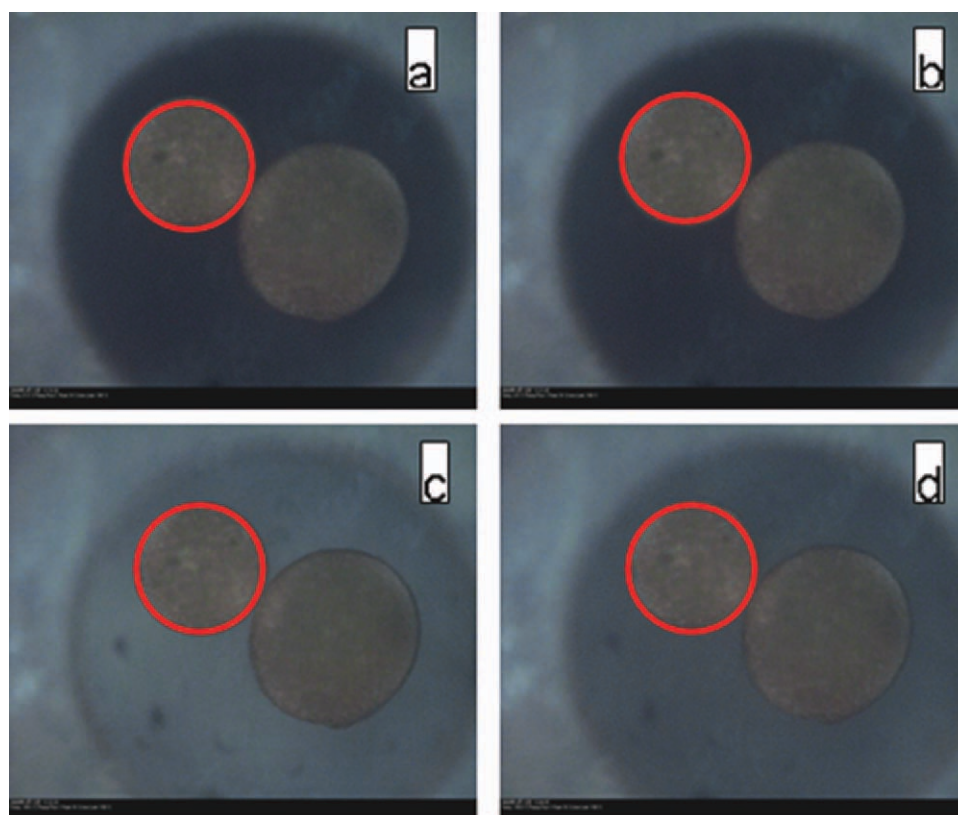


Figure 14 Topography of PIEK hollow microspheres under cold environment (a: 21.3°C, b: -0.5°C, c: -106.3°C, and d: -190°C) [Color figure can be viewed in the online issue, which is available at wileyonlinelibrary.com].

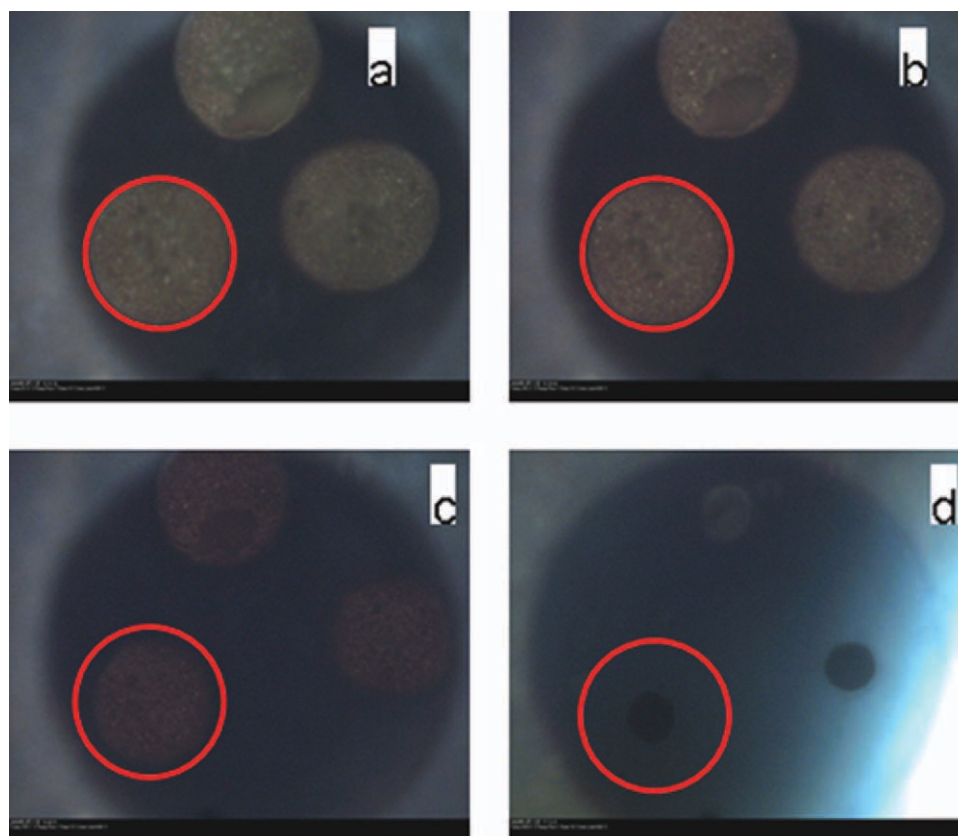


Figure 15 Topography of PIEK hollow microspheres under high temperature (a: 52.5°C, b: 283.2°C, c: 354.2°C, d: 600°C) [Color figure can be viewed in the online issue, which is available at wileyonlinelibrary.com].

TABLE VI
Inflation Pressure of PIEK Hollow Microspheres (atm) PIEK Hollow Microspheres were Filled with Nitrogen to Determine the Maximum Bearing Pressure

| Wall thickness | 1# | 2# | 3# | 4# | 5# | 6# | 7# | Average value |
|------------------|------|------|------|------|------|------|------|---------------|
| 10 μm | 0.70 | 0.65 | 0.52 | 0.74 | 0.61 | 0.59 | 0.68 | 0.64 |
| 20 μm | 1.87 | 1.56 | 1.57 | 1.66 | 0.95 | 1.15 | 1.52 | 1.47 |
| 40 μm | 3.30 | 3.02 | 3.36 | 3.68 | 4.77 | 3.38 | 3.83 | 3.62 |

properties of PIEK hollow microspheres suggested that they might have potential practical values in ICF pellet.

References

- McQuillan, B. W.; Nikroo, A.; Steinman, D. A.; Elsner, F. H.; Czechowicz, D. G.; Hoppe, M. L.; Sixtus, M.; Miller, W. J. *Fusion Sci Technol* 1997, 31, 281.
- Nuckolls, J.; Wood, L.; Hiessen, A. *Nature* 1972, 239, 139.
- Koopmans, J. R.; Paquet, A. N. *Adv Mater* 2000, 23, 1873.
- Nikroo, A.; Elsner, F. H.; Czechowicz, D. G. *Proc of 1st Inertial Fusion Sciences and Applications, Bordeaux, Elsevier Press*, 2001.
- Paguio, R. R.; Nikroo, A.; Takagi, M. *J Appl Polym Sci* 2006, 101, 2523.
- Sharma, M.; Rao, I. M.; Bijwe, J. *Wear* 2009, 267, 839.
- Akamatsu, K.; Ikeda, S.; Nawafune, H.; Yanagimoto, H. *J Am Chem Soc* 2004, 126, 10822.
- Kumara, S.; Ratha, T.; Mahalinga, R. N.; Reddy, C. S.; Dasa, C. K.; Pandey, K. N.; Srivastava, R. B.; Yadaw, S. B. *Mater Sci Eng B* 2007, 141, 61.
- Bee, T. L.; Chung, T. S.; Chen, H. M. *Macromolecules* 2009, 42, 7042.
- Hendrik, F.; Ulrich, Z.; Katharima, L. *Macromolecules* 2009, 42, 7846.
- Chang, G. J.; Luo, X.; Zhang, L.; Lin, R. X. *Macromolecules* 2007, 40, 8625.
- Nagai, K.; Norimatsu, T.; Lzawa, Y. *Encyclopedia of Nanoscience and Nanotechnology* 2004, 4, 407.
- McQuillan, B. W. *Fusion Technol* 1997, 31, 381.
- Norimatsu, T.; Nagai, K. *Fusion Eng Des* 2002, 63, 587.
- Nisisako, T.; Okushima, S.; Torii, T. *Soft Matter* 2005, 1, 23.